

## Differential reflection spectroscopy of a single quantum dot strongly coupled to a photonic crystal cavity

Erik D. Kim,<sup>1,a)</sup> Arka Majumdar,<sup>1</sup> Hyochoi Kim,<sup>2</sup> Pierre Petroff,<sup>2</sup> and Jelena Vučković<sup>1</sup>

<sup>1</sup>*E. L. Ginzton Laboratory, Stanford University, Stanford, California 94305, USA*

<sup>2</sup>*Department of Electrical and Computer Engineering, University of California, Santa Barbara, California 93106, USA*

(Received 8 May 2010; accepted 2 July 2010; published online 4 August 2010)

We demonstrate the use of periodically modulated Coulomb shifts in quantum dot (QD) transition energies to obtain differential reflection spectra of a photonic crystal nanocavity containing strongly coupled dots. Measured spectra isolate the change in the empty cavity optical reflectivity spectrum due to the presence of each dot. This technique permits the probing of coupled QD-cavity systems possessing cavity modes of arbitrary polarization, making it attractive for use in both cavity quantum electrodynamics studies and quantum information applications. © 2010 American Institute of Physics. [doi:10.1063/1.3469922]

Optical cavities containing atomic or atom-like emitters are attractive systems for cavity quantum electrodynamics (QED) studies<sup>1–4</sup> as well as for quantum information applications where strong light-matter interactions are desired.<sup>5–8</sup> The strongly enhanced interaction between the modes of a high quality factor photonic crystal cavity (PCC) (Ref. 9) and a quantum dot (QD) (Refs. 4 and 10) provides the prospect of naturally scalable quantum networks based on photonic crystal structures and QDs.<sup>6</sup> The ability to optically probe this enhanced interaction with high sensitivity is vital to accurately determine system parameters, observe cavity QED phenomena and perform the read-out operations required for quantum computing applications.<sup>11</sup>

Typically, coupled QD-cavity spectra are measured either incoherently in photoluminescence (PL) studies<sup>4</sup> employing a carrier-generating above-band laser or coherently in cross-polarized cavity reflectivity measurements<sup>10</sup> performed by scanning the frequency of a narrow-bandwidth continuous wave (cw) laser across the cavity resonance. In PL studies, observed spectra can be complicated by the presence of uncoupled QDs emitting light at frequencies near the cavity resonance. In cross-polarized reflectivity measurements, spectra are equivalent to those that would be obtained in transmission measurements for a configuration where the sample is placed in a rotatable mount between two cross-polarized linear polarizers to prevent transmission of incident light that does not interact with the linearly polarized cavity. Though this approach provides a means of measuring spectra directly, it is hampered by the limited extinction ratios of the polarizing elements used to minimize signal background. Further, the cross-polarized technique imposes the constraint that the incident light be neither parallel nor orthogonal to the cavity mode polarization, preventing it from being used to probe coupled QD-cavity systems possessing cavity modes of more general polarization.

Here, we perform coherent optical spectroscopy of the strongly coupled QD-PCC system by directly measuring the change in the empty cavity reflectivity spectrum arising from QD-cavity coupling. Our approach relies on the Coulomb shifting of a dot's optical transition energy that occurs when

carriers (e.g., electrons and holes) generated by an above-band laser are captured in it. Modulation of this Coulomb shift, achieved by modulating the above-band laser amplitude, enables phase-sensitive differential reflection (DR) measurements of coupled QD-cavity spectra. Further, implementation of homodyne detection techniques removes the restriction of such measurements to linearly polarized optical cavities.

Studies are performed on individual self-assembled InAs QDs coupled to an “L3” linear three-hole defect GaAs photonic crystal nanocavity.<sup>9</sup> The QDs are grown by molecular beam epitaxy on a GaAs substrate and positioned at the center of a 164 nm thick GaAs membrane. The photonic crystal cavities are fabricated in the membrane through a procedure involving electron beam lithography, reactive ion etching, and hydrofluoric acid wet-etching of the AlGaAs sacrificial layer beneath the membrane, as described previously.<sup>10</sup> Samples are placed in a liquid He flow cold-finger cryostat enabling operating temperatures of 5–40 K. A microscope objective (0.75 numerical aperture) serves both to focus optical fields (incident along an axis normal to the photonic crystal plane) onto the sample and to collect light reflected from the 10-period quarter-wave distributed Bragg reflector (DBR) located approximately 1  $\mu\text{m}$  below the GaAs membrane.

The experimental setup employed in DR studies is shown in Fig. 1(a). The use of a nonpolarizing beam splitter (NPBS) before the sample allows collection of the DBR-reflected light that does not interact with the cavity. This enables homodyne measurements that both provide improved contrast in obtained reflectivity spectra<sup>12</sup> and allow copolarized optical excitation of the cavity mode. A 780 nm cw laser modulated by an acousto-optic modulator (AOM) serves to generate carriers in the GaAs membrane that relax into the QDs and Coulomb shift their optical transition energies by a few to several millielectronvolt depending on the carrier(s) captured.<sup>13</sup> Therefore, square-wave modulation of the 780 nm cw laser at frequencies much smaller than the carrier relaxation rates modulates the cavity reflectivity spectrum between the empty cavity case and the case where the QD transition energy is near the cavity resonance, since the capture-induced QD Coulomb shifts are much larger than

<sup>a)</sup>Electronic mail: erikdkim@stanford.edu.

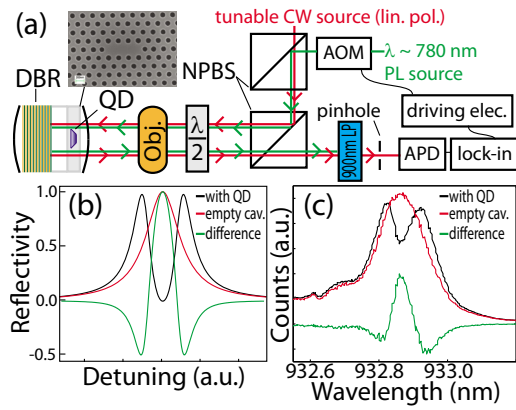


FIG. 1. (Color online) (a) Experimental setup employing a NPBS for homodyne measurements. The carrier-generating 780 nm cw field is modulated with an AOM to enable phase sensitive detection with an APD and a lock-in amplifier. A half-wave plate ( $\lambda/2$ ) is used to ensure that the linearly polarized scanning cw laser and cavity mode are copolarized, while a microscope objective (Obj.) focuses incident light onto the sample. A scanning electron micrograph of the L3 cavity is shown in the inset. (b) Theoretical and (c) experimentally obtained cavity reflectivity spectra with and without a resonant QD. The calculated difference between the two spectra in each case is also given. Theoretical plots ignore the effects of spectral wandering and blinking. Experimental spectra were obtained in cross-polarized reflectivity measurements without the use of phase-sensitive techniques as in Ref. 10.

typical PCC linewidths ( $\sim 0.1$  meV). This modulation enables the use of lock-in detection techniques to directly measure the DR spectrum  $\Delta R(\omega) = R_{\text{off}}(\omega) - R_{\text{on}}(\omega)$  as a function of laser frequency  $\omega$ , where  $R_{\text{off}}(\omega) = |\kappa/[i(\omega_c - \omega) + \kappa]|^2$  is the empty cavity reflectivity spectrum centered at  $\omega_c$  and  $R_{\text{on}}(\omega) = |\kappa/\{i(\omega_c - \omega) + \kappa + g^2/[i(\omega_{\text{QD}} - \omega) + \gamma]\}|^2$  is the cavity reflectivity spectrum in the presence of a coupled QD at  $\omega_{\text{QD}}$  for vacuum Rabi frequency  $g$ , QD dephasing rate  $\gamma$ , and cavity field decay rate  $\kappa$ .<sup>10</sup>

Figure 1(b) plots theoretically calculated reflectivity spectra with and without a resonantly coupled QD as well as the difference  $\Delta R$ . In these plots, the effects of spectral wandering and QD blinking are ignored, leading to a dipole-induced transparency “dip” in the reflectivity spectrum of a cavity containing a coupled QD that nearly approaches zero between the polariton peaks.<sup>14</sup> Figure 1(c) plots corresponding experimental cavity reflectivity traces obtained in standard cross-polarized reflectivity measurements<sup>10</sup> without phase-sensitive techniques. In the experimental case, the reflectivity dip is significantly diminished by the effects of spectral wandering and blinking,<sup>15</sup> limiting the difference spectrum contrast. We also note that the signal-to-noise ratio (SNR) in these measurements suffers from imperfect extinction ratios of polarization optics and  $1/f$  noise associated with these essentially dc measurements. As such, the phase-sensitive homodyne measurements employed in DR spectroscopy offer a means of overcoming both limitations.

To obtain DR spectra, we scan the tunable, linearly polarized cw field through the cavity resonance and collect both the cavity and DBR reflected fields while modulating the QD in and out of resonance with the cavity via the modulated 780 nm laser. These fields interfere on the surface of an avalanche photodiode (APD) whose photocurrent is measured by a lock-in amplifier operating at the AOM modulation frequency. 780 nm light is prevented from reaching the APD by the use of a 900 nm long-pass optical filter. Lock-in measured DR spectra for different QD-cavity detunings are

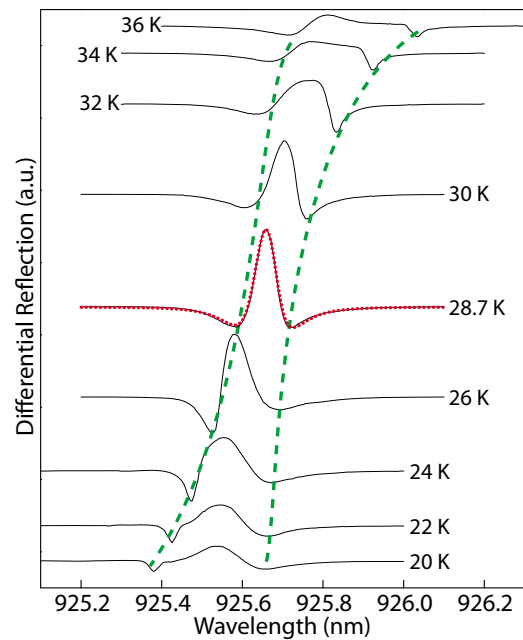


FIG. 2. (Color online) DR spectra (offset) obtained at different sample temperatures with a 6 nW tunable cw laser and a 20 nW 780 nm laser modulated at 20 kHz. Temperature variation serves to tune the QD through the cavity resonance. The dotted curve is a fit of the analytical expression for  $\Delta R$  to the 28.7 K trace. The two dashed lines are guides to the eye to show the anti-crossing of the polariton peaks corresponding roughly to the minimum values in each spectrum.

shown in Fig. 2 for a QD different from the one used in Fig. 1(c). In each trace, the tunable and 780 nm cw sources are kept at 6 nW and 20 nW, respectively (as measured before the microscope objective), with the latter modulated at 20 kHz. The QD-cavity detuning is varied by controlling the sample temperature, showing the anti-crossing of the polariton peaks as the QD is tuned across the cavity resonance. A fit of  $\Delta R$  to the data obtained at 28.7 K yields a vacuum Rabi frequency  $g/2\pi = 20.5 \pm 0.2$  GHz and a cavity field decay rate  $\kappa/2\pi = 38.3 \pm 0.7$  GHz, consistent with previous studies in similar samples.<sup>10,15</sup>

We emphasize that the shifting of QD energies utilized in our technique arises from the capture of carriers generated by the 780 nm laser into the QD rather than from a dc Stark shift caused by the electric field of carriers captured in the GaAs membrane and in nearby QDs. In the latter case, for low 780 nm laser powers inducing dc Stark shifts smaller than the cavity linewidth, the DR spectrum would take the form of the derivative of the coupled QD-cavity spectrum [e.g., the derivative of the black curve in Fig. 1(c) for a QD tuned to the cavity resonance]. Increasing the laser power would lead to higher signal strengths and the eventual emergence of two identical (but inverted) spectral features centered at the QD energy and separated by the dc Stark shift energy.<sup>16</sup>

To verify the Coulomb shifts, we obtained DR spectra at different laser powers for a QD tuned near the cavity resonance. Results are shown in Fig. 3 for a modulation frequency of 10 kHz and a 20 nW tunable cw laser. We find that the DR spectra maintain the same qualitative form as the 780 nm laser power is increased, with the signal strength—defined as the difference between maximum and minimum values in each spectrum—saturating at higher powers. This saturation is expected as it occurs when the rate of carrier

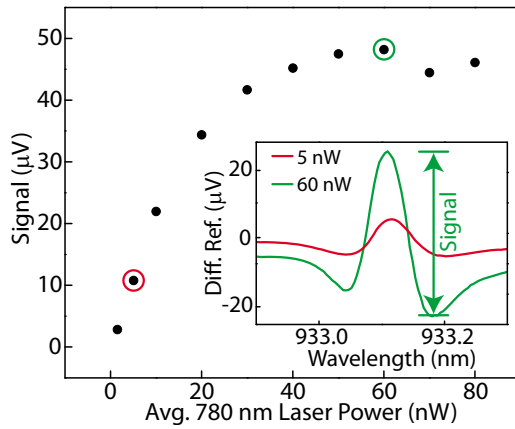


FIG. 3. (Color online) Signal strengths in DR spectra as a function of 780 nm laser power for a QD resonant with a PCC. The tunable cw laser is kept at 20 nW and the 780 nm laser is modulated at 10 kHz. The signal is taken as the difference between maximum and minimum values in each DR spectrum and is shown to saturate at higher powers. Inset: DR spectra for 780 nm laser powers of 5 nW and 60 nW.

capture into QDs approaches the carrier relaxation rate. We observe neither a derivative type signal at lower powers nor the emergence of two separate spectral features as the power is increased. These results substantiate the claim that carrier capture is the primary mechanism by which QD energies are shifted. Further, these results reveal the achievable SNR in DR spectroscopy. Using the standard deviation of data points measured when the tunable cw laser is highly detuned from the cavity as a figure of noise, we obtain a maximum SNR of  $\sim 900$  for a 50 nW 780 nm field. This value is nearly an order of magnitude greater than the SNR of  $\sim 100$  obtained in cross-polarized reflectivity measurements of the same QD. As the SNR depends on the effects of spectral wandering and blinking, values will generally vary from dot to dot and will be higher in QDs where these effects are reduced.

In summary, we have performed coherent optical spectroscopy on the strongly coupled QD-PCC system through measurements of DR spectra. Our experimental technique is highly suited for studies of cavity QED phenomena where high SNR is crucial and should in principle be applicable to

quantum information processing protocols proposing the use of QD spins in circularly polarized optical cavities.<sup>5</sup> Further, the principle of this technique may also be applied to time-domain studies of QDs strongly coupled to optical cavities, where optical pulses would be used instead of the scanning cw field, allowing the observation of transient phenomena.

This work was supported in part by NSF (DMR-0757112), DARPA (N66001-09-1-2024), ARO (54651-PH), and ONR (N00014-08-1-0561). E.K. was supported by the IC Postdoctoral Research Fellowship. A.M. was supported by the Texas Instruments Fellowship.

- <sup>1</sup>R. J. Thompson, G. Rempe, and H. J. Kimble, *Phys. Rev. Lett.* **68**, 1132 (1992).
- <sup>2</sup>A. Wallraff, D. I. Schuster, A. Blais, L. Frunzio, R.-S. Huang, J. Majer, S. Kumar, S. M. Girvin, and R. J. Schoelkopf, *Nature (London)* **431**, 162 (2004).
- <sup>3</sup>J. P. Reithmaier, G. Sek, A. Löffler, C. Hofmann, S. Kuhn, S. Reitzenstein, L. V. Keldysh, V. D. Kulakovskii, T. L. Reinecke, and A. Forchel, *Nature (London)* **432**, 197 (2004).
- <sup>4</sup>T. Yoshie, A. Scherer, J. Hendrickson, G. Khitrova, H. M. Gibbs, G. Rupper, C. Ell, O. B. Shchekin, and D. G. Deppe, *Nature (London)* **432**, 200 (2004).
- <sup>5</sup>A. Imamoglu, D. D. Awschalom, G. Burkard, D. P. DiVincenzo, D. Loss, M. Sherwin, and A. Small, *Phys. Rev. Lett.* **83**, 4204 (1999).
- <sup>6</sup>A. Faraon, I. Fushman, D. Englund, N. Stoltz, P. Petroff, and J. Vučković, *Opt. Express* **16**, 12154 (2008).
- <sup>7</sup>H. J. Kimble, *Nature (London)* **453**, 1023 (2008).
- <sup>8</sup>L. DiCarlo, J. M. Chow, J. M. Gambetta, L. S. Bishop, B. R. Johnson, D. I. Schuster, J. Majer, A. Blais, L. Frunzio, S. M. Girvin, and R. J. Schoelkopf, *Nature (London)* **460**, 240 (2009).
- <sup>9</sup>Y. Akahane, T. Asano, B.-S. Song, and S. Noda, *Nature (London)* **425**, 944 (2003).
- <sup>10</sup>D. Englund, A. Faraon, I. Fushman, N. Stoltz, P. Petroff, and J. Vuckovic, *Nature (London)* **450**, 857 (2007).
- <sup>11</sup>D. P. DiVincenzo, *Fortschr. Phys.* **48**, 771 (2000).
- <sup>12</sup>K. Karrai and R. J. Warburton, *Superlattices Microstruct.* **33**, 311 (2003).
- <sup>13</sup>R. J. Warburton, C. S. Durr, K. Karrai, J. P. Kotthaus, G. Medeiros-Ribeiro, and P. M. Petroff, *Phys. Rev. Lett.* **79**, 5282 (1997).
- <sup>14</sup>E. Waks and J. Vuckovic, *Phys. Rev. Lett.* **96**, 153601 (2006).
- <sup>15</sup>I. Fushman, D. Englund, A. Faraon, N. Stoltz, P. Petroff, and J. Vuckovic, *Science* **320**, 769 (2008).
- <sup>16</sup>B. Alén, F. Bickel, K. Karrai, R. J. Warburton, and P. M. Petroff, *Appl. Phys. Lett.* **83**, 2235 (2003).